Calculation of Torsional Vibrations and Prediction of Print Quality in Sheetfed Offset Printing Presses

N. Norrick, S. Neeb

In sheetfed offset printing presses the synchronous drive of the paper-carrying cylinders is achieved by a continuous geared drive train. Due to the mechanical compliance of the drive train, the system is capable of torsional oscillations, which are excited by a multiplicity of phenomena. The oscillations of the gear train have a direct effect on print quality. The color register must not fluctuate from sheet to sheet, since fluctuations on the order of a few μm lead to unacceptable printing results. The excitation frequencies or orders in the printing press lead to register errors with corresponding orders on the printed sheets. Using a mechanical model of the printing press, the effects of the excitations on the system can be simulated and, thus, predictions of register variation can be made using a sheet-tracking algorithm. In a practical example, it is shown how due to a harmonic disturbance acting on the main drive motor, register variations occur with a corresponding rhythm. By compensating the excitation (feed-forward control), the torsional vibrations of the machine can be suppressed and the print quality can thus be ensured. This is shown both in the simulation and on the basis of measured data. It is thus possible to predict the effect of mechanical or control-related changes in the design of the printing machine, which ultimately saves time and money during machine development and manufacturing.

1 Introduction

Sheetfed offset printing presses offer high print quality due to the exact hand-over of sheets from one inking unit to the next (Kipphan, 2000). The exact hand-over of sheets at high speeds of up to 18000 sheets/hour (corresponding to five sheets/s or 7.6 m/s sheet velocity for the machine type discussed in this paper) is attained by using cam-driven grippers. A continuous geared drive drain connects the paper-carrying cylinders. This drive train is powered by a single electric main drive motor. In this way, sheets can be transported through machines with lengths of 30 m or more with errors on the order of 10 μm. The cutaway view in Figure 1 shows the cylinder layout as well as important components of a modern large format printing press (sheet format up to 1210 mm × 1620 mm) with six inking units and one varnishing unit (Heidelberg Speedmaster XL162-6+L). The sheets are taken from a paper pile in the feeder (on the right) and accelerated to machine speed, then transported through the machine via grippers, printed with multiple colors on the way, and dried and piled in the delivery (on the left).
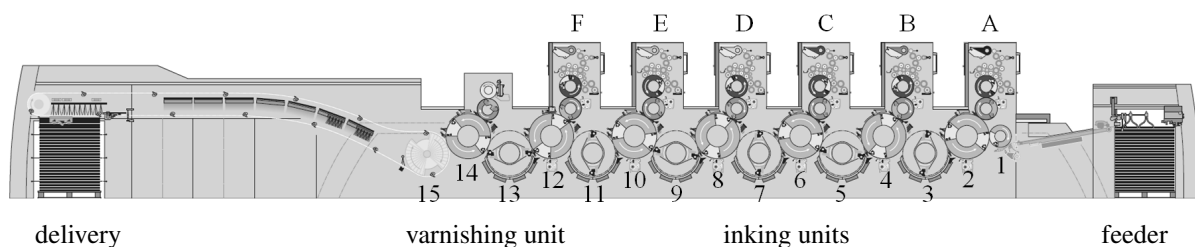

Figure 1. Cutaway view of a Heidelberg Speedmaster XL162-6+L sheetfed offset printing press with six inking units (marked A to F), one varnishing unit and 15 degrees of freedom (marked 1 to 15). The degrees of freedom of the main drive motor and the intermediate gear are not shown. Paper feed direction is from right to left.

Due to the mechanical compliance of the gear coupling, the printing machine is a system capable of torsional oscillation, which is excited by a multiplicity of phenomena. In addition to the reaction torques of the aforementioned gripper mechanisms, examples of predominant excitations are the drive belt (Langer, 2013; Messer, 2013), the

vibrating roller for ink transport (Hummel et al., 1998; Heiler and Hieronymus, 2009), and the rotary encoder of the main drive. In the following, these three excitation mechanisms are briefly described:

a) Drive belt: Due to the manufacturing process of the drive belt, the transmission ratio fluctuates during one belt circumference as described by Langer (2013). This results in an oscillation of the driving torque. The excitation is periodic with respect to the belt loop, allowing it to be divided into harmonic parts using Fourier analysis. These harmonics correspond to non-integer machine orders when calculated in machine coordinates due to the non-integer transmission ratio.

b) Vibrating roller for ink transport: The vibrating roller is an integral part of each inking unit and responsible for the transport of ink from the ink supply fountain into the inking unit. The roller oscillates back and forth between the ductor roller, where it receives ink, and the first ink roller, where it expends ink into the inking unit. It is not driven so that it must be re-accelerated to machine speed at every stroke. This provides a shock-like excitation for the machine, which responds with harmonic vibrations at non-integer machine orders.

c) Rotary encoder of the main drive motor: The errors of the rotary encoder mounted to the shaft of the main drive motor are passed on to the machine via the motor control. The excitation mechanism will be explained in detail in section 4.

The excited torsional vibrations have a direct effect on the printing quality, since the individual colors are transferred successively to the sheet during multicolor printing, but the positions of the colors must match exactly. The correlation of the independently printed colors is called color registration or register. Only minimal variations of the color register from sheet to sheet are tolerable, whereby fluctuation amplitudes of a few µm lead to unacceptable printing results. The excitation frequencies or orders in the printing press can be found as register variations with corresponding orders on the printed sheets. It is a prime example of (inevitable) undersampling: High frequency vibrations of the machine, e.g. the effect of the vibrating roller with an excitation order $f_o = 2.\overline{3}$ are sampled with one sheet per machine revolution (sampling frequency $f_s = 1$). After a Fast-Fourier-Transform (FFT) into the order domain aliasing leaves us with an amplitude error at the order 0.x because of the formula

$$f_{\text{alias,principal}} = \min |f_o - N f_s| \qquad N \in \mathbb{N}, \tag{1}$$

which yields an order of $0.\overline{3}$ in the current example. Figure 2 shows the connection between the machine vibration, the sampling with one sheet per machine revolution and the transformation of the signal into the order domain. Although an error is made due to undersampling, important information can be obtained from the analysis of the register data.
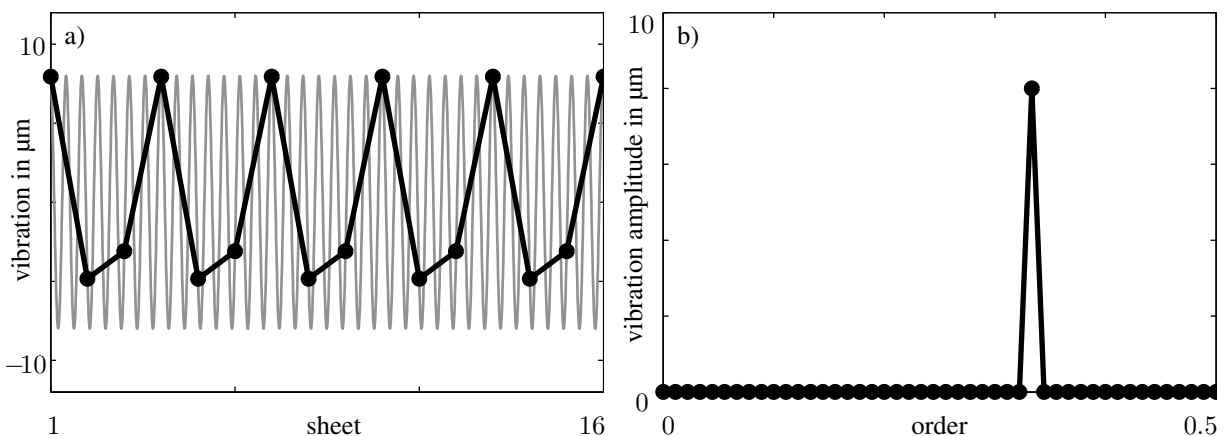

Figure 2. a) High-frequency vibrations of the machine (thin gray curve, machine order $2.\overline{3}$) are sampled with one sheet per machine revolution (black dots). b) Sheet signal transformed into the order domain.

In this context it is important to note that vibrations at integer orders do not result in register variation since they are always sampled at the same phase angle. This is the case, for example, for the reaction torques of the gripper systems. Vibrations with non-integer orders, on the other hand, such as the aforementioned mechanisms, produce disturbances in the printed image.

In the case of web printing machines, a large number of publications dealing with the modeling of the printing machine and the prediction of registration values can be found. A comprehensive process model for web printing was derived for the first time in the 1970s in the groundbreaking works of Brandenburg (1971, 1976) . Publications from various research groups followed. This trend has continued up to the present day, as shown by more current research papers (Wolfermann, 1995; Zitt, 2001; Galle, 2007; Schnabel, 2009; Brandenburg, 2011). The overall aim is always dynamic and precise control of print quality in order to increase productivity while at the same time minimizing energy and raw material use. In the case of sheetfed printing presses, this broad basis of publications is missing, although the objectives are fundamentally the same. This paper is one building block in the filling of this gap.

Using a mechanical model of the printing press, the effects of the excitations on the system can be simulated and, with a suitable post-processing algorithm, predictions of register variation can be calculated. The mechanical model and the post-processing algorithm for the prediction of register variation are explained in detail in the following two sections.

2 Mechanical Modeling

Torsional vibration models of the complete printing press have been used for many years to aid in the understanding and design of sheetfed offset printing press dynamics (Buck et al., 2005; Wiese, 1998; Norrick, 2015). Naturally, the necessary modeling depth and complexity are different depending on the questions that need to be answered.

For this work, a discrete torsional degree of freedom (DoF) q_n is assigned for each paper-carrying cylinder. In addition, degrees of freedom are assigned to the drive motor and the intermediate gear. The moments of inertia can be calculated from CAD models of the assembled components. The moments of inertia of the other cylinders and rollers in each printing unit are added to the corresponding printing cylinder. The coupling of the DoF is attained by discrete spring-damper elements which also include the nonlinearity due to gear tooth clearance (backlash). Because of this, the spring-damper elements are dependent on the relative angular position of adjacent cylinders Δq. A schematic of the discrete modeling incorporating backlash is shown in Figure 3. Stiffness and damping values can be evaluated by model updating using measured machine natural frequencies and modal damping.
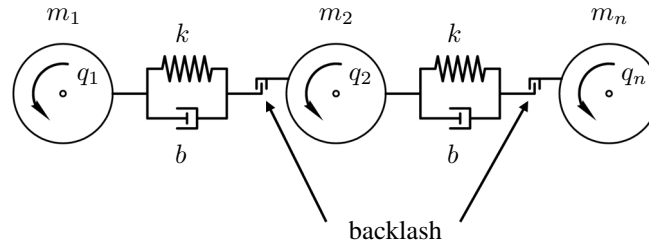

Figure 3. Schematic of the discrete modeling incorporating backlash.

The system equations in matrix form are

$$\boldsymbol{M}\ddot{\boldsymbol{q}} + \boldsymbol{B}(\Delta\boldsymbol{q})\,\dot{\boldsymbol{q}} + \boldsymbol{K}(\Delta\boldsymbol{q})\,\boldsymbol{q} = \boldsymbol{T}\,, \tag{2}$$

with $\boldsymbol{M}$ being the mass matrix, $\boldsymbol{B}$ being the damping matrix and $\boldsymbol{K}$ being the stiffness matrix. The vector of excitation torques $\boldsymbol{T}$ is described by

$$\boldsymbol{T} = \boldsymbol{T}_A(\boldsymbol{q},\dot{\boldsymbol{q}}) + \boldsymbol{T}_G(\boldsymbol{q},\dot{\boldsymbol{q}}) - \boldsymbol{T}_R(\dot{\boldsymbol{q}})\,. \tag{3}$$

$\boldsymbol{T}_A$ is the torque from the main motor control, which is only applied to the DoF of the motor. Input values for the motor feedback control are machine angle and machine angular velocity. The control strategy is a cascade control with a proportional (P-) position control and a PI-velocity control. The filtering of the input signals and the signal delay times are accounted for, since these influence the system behavior.

$\boldsymbol{T}_G$ are the reaction torques of the gripper cams which are dependent on machine angle and angular velocity. The torque values are gained from kinetostatic analysis or detailed multibody simulations, e.g. MSC/ADAMS.

$\boldsymbol{T}_R$ is the speed-dependent friction torque which is known from many measurements and distributed on the DoF

according to the machine configuration. For example, a printing unit and a varnishing unit have different friction torque values.

The calculation is carried out in the time domain utilizing Matlab/Simulink. To manage the large number of possible machine configurations it is of the utmost importance to ensure a well-structured and automated design of the models.

For the case that the machine behavior is linear, i.e. no backlash occurs during operation, the complex transfer function between the torque of the main drive motor and the relative cylinder rotation

$$\underline{H}(\Omega) = \frac{q_{12} - q_2}{T_A} \tag{4}$$

can be measured as well as calculated from the model. Figure 4 shows the amplitude and phase curves of measured transfer functions for seven printing presses of the same configuration and the comparison with the simulated transfer function for the same configuration. The coherence function γ^2 (as defined by Markert (2013)) gives us information about the reproducibility of the system's behavior. Where the transfer function amplitudes are significant, the coherence is near 1, making it obvious that the system behavior from one machine to the next is reproducible. In addition it is evident that the natural frequencies and modal damping of the mechanical model fit the measured values very well.
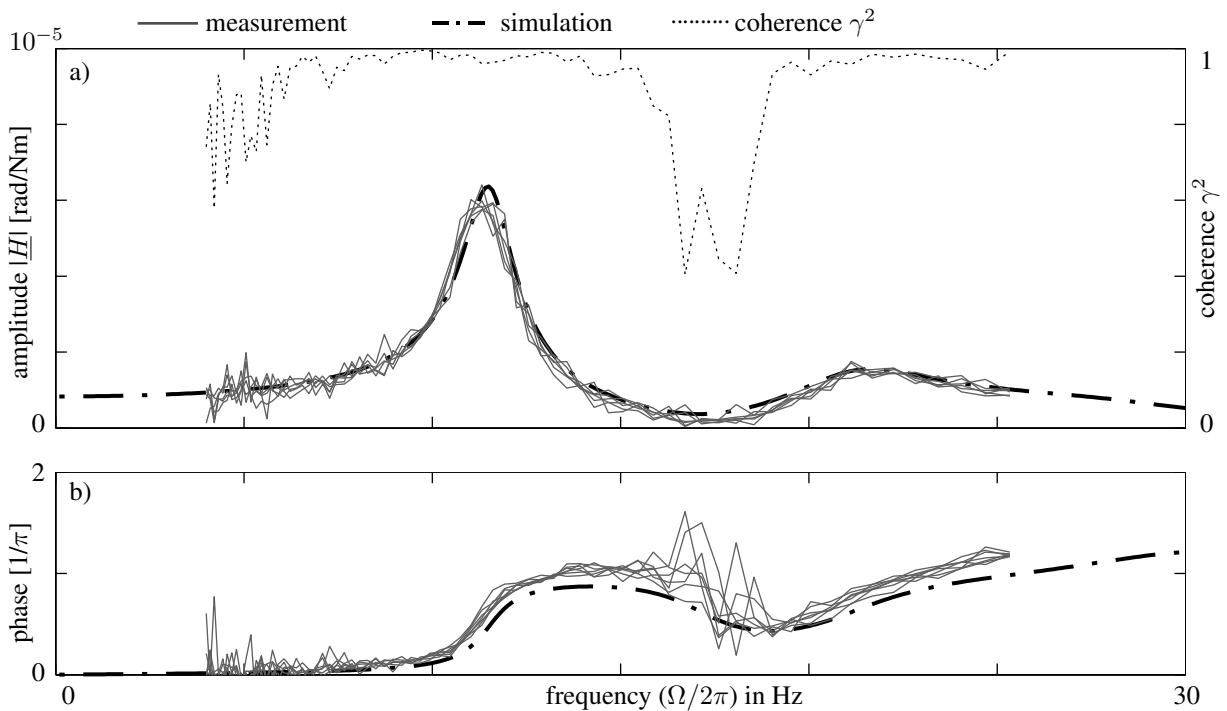

Figure 4. Comparison of measured transfer functions for seven printing presses of the same configuration and simulated transfer function (amplitude (a) and phase (b)) as well as the coherence function γ^2 (reproduced from Norrick, 2015).

3 Post-Processing: Sheet-tracking Algorithm

To predict print quality, starting point is the calculated machine vibration for the operating point of interest. To calculate print quality during stationary operation it is sufficient to simulate the steady state vibrations at a constant printing speed. The algorithm presented here is not limited to steady state operation though, but also suited for transient operation such as emergency stop scenarios.

Preliminary results are rotation angle data for all paper-carrying cylinders at simulation time points ($q_n(t)$). The handover angles, i. e. the nominal cylinder angles at which the sheet transfer takes place, are part of the machine design and known for a certain machine. To track a sheet through the machine, the following steps must be taken: First, for n paper-carrying cylinders the points in time are calculated at which the cylinder angles are equal to the

handover angles. If necessary, interpolation between simulation time points yields more exact results. Next, from this matrix of handover times, the points in time are extracted that correspond to a certain sheet moving through the machine. Then, for each of the $n-1$ handovers, the difference between the rotation angle of the "giving" cylinder $n-1$ and the "receiving" cylinder n is calculated. The receiving cylinder is used as a reference. The giving cylinder hands the sheet over too early or too late, depending on the state of vibration of the machine. The angle-based handover errors multiplied by the cylinder radius r are converted into circumferential handover errors u. Finally, the cumulative handover error can be calculated which is equal to the color register from one printing unit to the next. The color register values can be specified relative to the first printing unit or as a register difference between neighboring units.

As an example, the machine model can be subjected to an excitation with the machine order $2.\overline{3}$. The simulation is carried out during steady state at printing speeds from 10000 to 14000 sheets/hour for time spans corresponding to 100 sheets. The time domain data are transferred to the sheet-tracking algorithm. Figure 5 shows the simulated machine vibrations at 12000 sheets/hour (relative vibration at the cylinder circumference between the first printing cylinder q_2 und the sixth printing cylinder q_{12}) as a time signal as well as the calculated register variation between printing unit one (DoF 2) and printing unit six (DoF 12) as a sheet signal as well as the values transformed into the order domain.
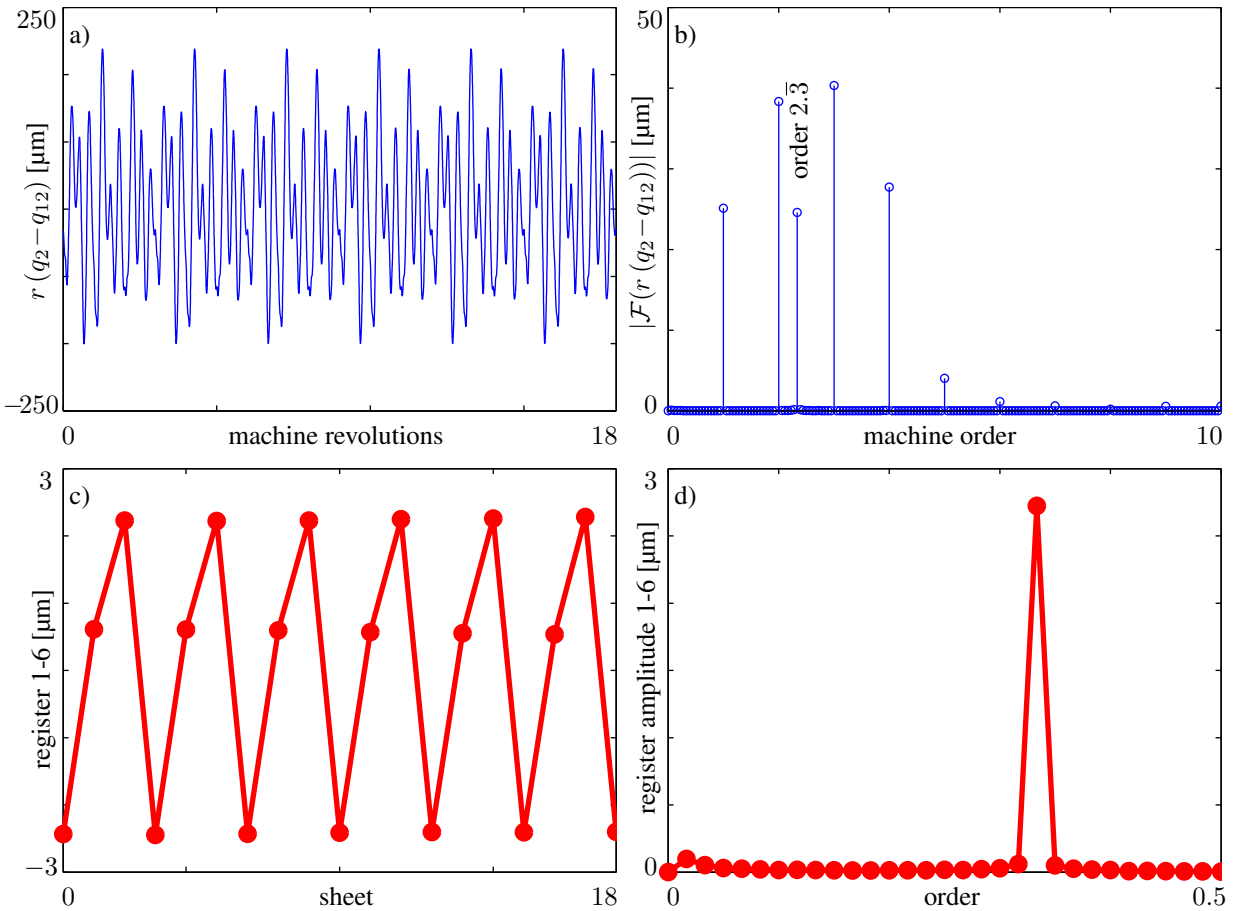

Figure 5. a) Calculated machine vibrations $r\,(q_2 - q_{12})$ in μm at a printing speed of 12000 sheets/hour, b) amplitude spectrum of the machine vibrations $|\mathcal{F}(r\,(q_2 - q_{12}))|$ in the order domain in μm at a printing speed of 12000 sheets/hour, c) Calculated color register variation in μm at a printing speed of 12000 sheets/hour, d) Order spectrum of the color register variation in μm at a printing speed of 12000 sheets/hour.

From the plots it is evident that the machine vibrations do not translate directly into register variations. The relative circumferential vibration of the printing cylinders is around $\pm 250\,\mu m$, but this results in only about $\pm 3\,\mu m$ of register variation. This has two reasons. First, only the non-integer machine order $2.\overline{3}$ is visible in the register variation, since integer machine orders have no effect on the register as detailed in section 1. Second, the sheets are not handed over at the vibration peaks (in general), but rather at various points of one oscillation. Depending on the mode shape or shapes being excited and the offset angle from one printing unit to the next, a superposition

takes place which can be positive or negative.

Figure 6 shows a summary of the results for the order $2.\overline{3}$ and $0.\overline{3}$, respectively, over printing speed. It is apparent that the vibration amplitudes of the machine and the register variation exhibit a maximum value around 12300 sheets/hour. This is due to resonance of the first elastic mode of the machine at 8 Hz, excited by the machine order $2.\overline{3}$ (12300 sheets/hour $\cong 3.42$ Hz; 3.42 Hz $\times 2.\overline{3} = 8$ Hz). Because the damping matrix is not diagonalizable, the mode shape is complex. The motions of the DoF are not in phase with each other, meaning the mode reaches its maximum value at different times for every location. The mode shape is visualized in Figure 7. The S-shape is characteristic of oscillator chains, as Dresig and Holzweißig (2009) have shown. The three-dimensional plot emphasizes the mode shape's twist in the complex plane.
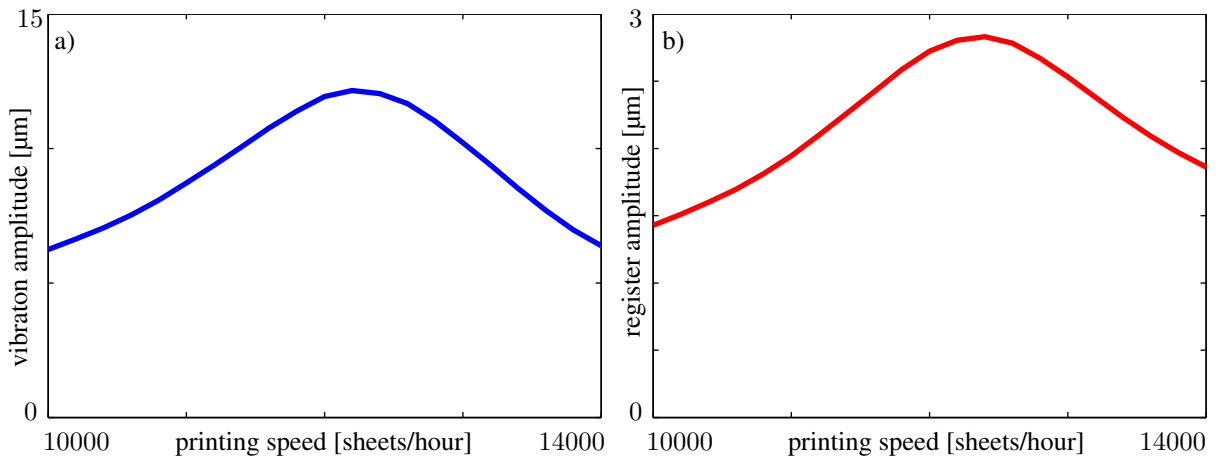

Figure 6. Calculated amplitude of the machine vibrations $r\,(q_2 - q_{12})$ at order $2.\overline{3}$ in μm for printing speeds from 10000 to 14000 sheets/hour, b) Calculated amplitude of the register variation at order $0.\overline{3}$ in μm for printing speeds from 10000 to 14000 sheets/hour.
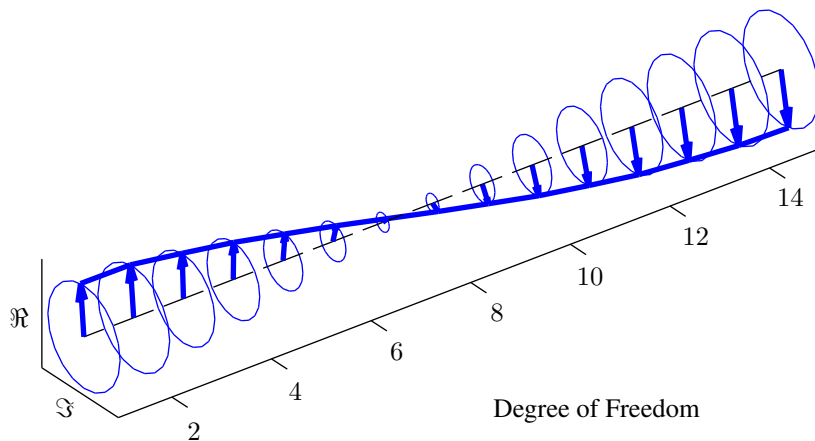

Figure 7. First elastic mode shape of the printing press at 8 Hz. The degrees of freedom of the main drive motor and the intermediate gear are not shown.

4 Example: Disturbance at the Main Drive Motor

A rotary encoder mounted to the shaft of the main drive motor of the printing press is used to generate the speed input signal for the motor control. Internal errors of the rotary encoder as well as external errors due to eccentric mounting of the encoder are responsible for modulating the encoder signal at constant speed with a harmonic error function. A pointer diagram (Figure 8a) shows the vector addition of internal and external encoder errors to a total error vector.

The frequency of this error function is visible in a motor torque variation, which in turn excites high-frequency
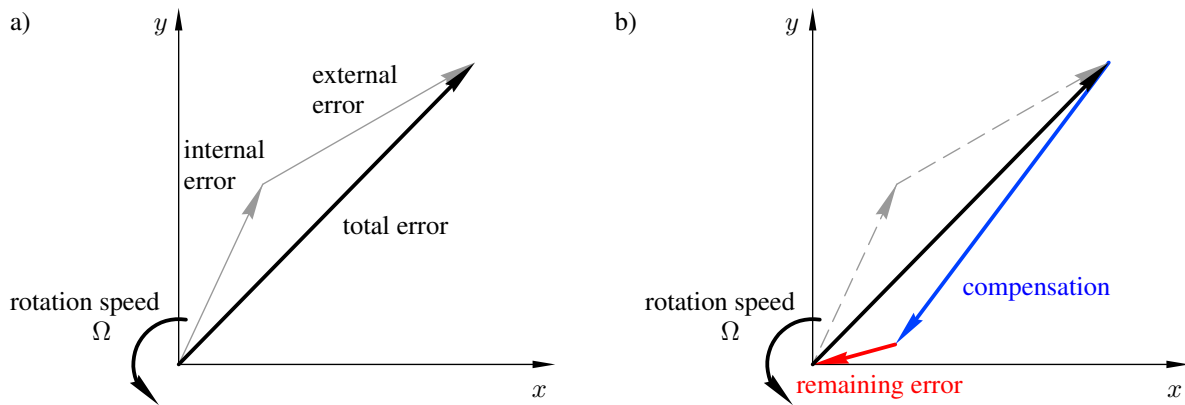
Figure 8. a) Summation of internal and external encoder errors to a total error vector. b) Remaining error after addition of the compensation signal.

vibrations of the printing press. Finally, these vibrations cause register variations with a corresponding rhythm on the printed sheets, leading to unacceptable print quality.

Measurements carried out on a Heidelberg Speedmaster XL162-6+L at a printing speed of 14200 sheets/hour show a variation in the motor torque T_A at machine order 10.06 – a non-integer value. On the printed sheets a register variation at the order 0.06 is visible, corresponding to the value calculated from equation (1). The register variation is mainly visible between printing units one and two. The measurement of the color register is done via optical acquisition of special measurement fields on the printed sheets. When observing the measurement instructions and good print quality in the single colors is given, the measurement uncertainty of this process reaches < 2 μm as detailed by the Polygraphische innovative Technik Leipzig GmbH (2016).

If the amplitude and phase values of the systematic error of the rotary encoder can be determined, the excitation can be compensated. In this way, the control does not "see" the eccentricity of the rotary encoder, so that the machine vibrations are not excited in the first place. Ideally, a signal with the exact amplitude and a phase angle shifted by π is added the the encoder signal. This would result in perfect compensation. Figure 8b shows a pointer diagram of the effect of the addition of a non-ideal compensation value, which corresponds to an error in the determined values of amplitude and phase angle.

The effectiveness of the compensation method can be demonstrated through simulation. In the model the encoder signal is superimposed by a sinusoidal disturbance with known amplitude and phase. Figure 9 shows the simulated amplitude spectra of the drive torque and the register variation without and with compensation of the encoder error. Naturally, when applying an ideal compensation in the model, there is no remaining error. Therefore, for the simulation results shown here, it was assumed that the value for the phase angle of the encoder error was incorrectly entered with $\Delta\varphi = 10°$, so that only an incomplete compensation of the error takes place. Since

$$|1 - e^{i\Delta\varphi}| \approx 0.83 \tag{5}$$

we expect a reduction of the motor torque vibration as well as the register variation of 83%, which is verified by the simulation.

With the help of the machine model, it is clear why the register error develops mainly between the first and second printing units: The order 10.06 excites a frequency of 40 Hz at 14200 sheets/hour. At this frequency, a mode shape of the machine is excited in which mainly the main drive motor and the first cylinders (degrees of freedom one to four) of the machine are involved. The eigenvector has hardly any deflections in the rear part of the machine, as shown in Figure 10.

The simulated behavior without and with compensation was tested on a real machine. The driving torque was recorded parallel to the printing of test sheets. After a first run without compensation, the compensation algorithm was activated in the main drive control and a second run with compensation was performed. In the measurements, a reduction of the driving torque fluctuation of 94% and a reduction of the register variation of 93% were achieved, as shown in Figure 11. In the amplitude spectrum of the drive torque it is evident that only the 10.06 is affected
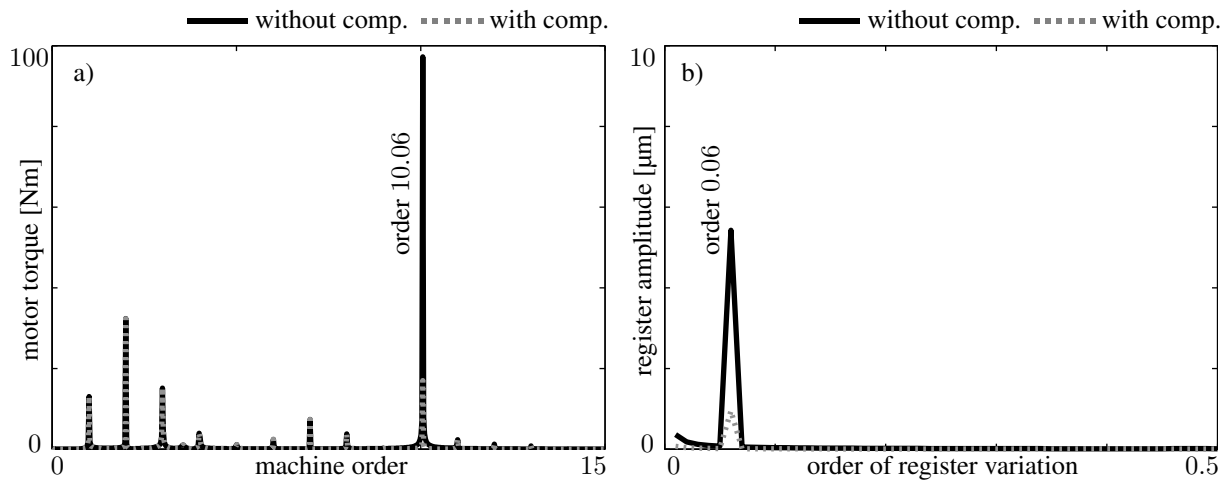
Figure 9. a) Calculated amplitude spectrum of the motor torque in machine coordinates [Nm] without and with compensation of the rotary encoder error. b) Calculated amplitude spectrum of the register variation from 100 consecutive sheets [μm] without and with compensation of the rotary encoder error.
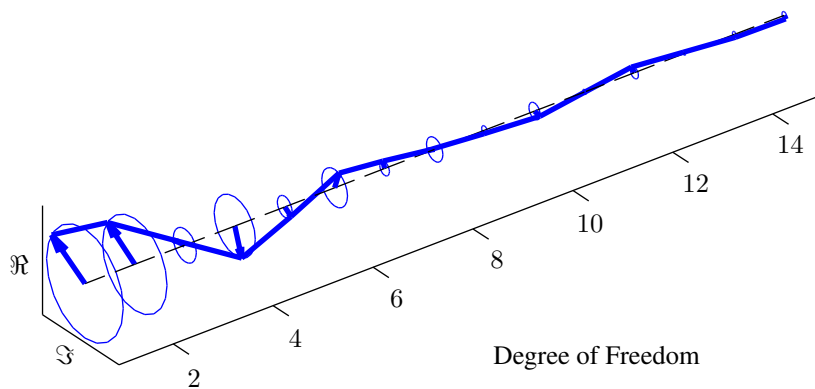

Figure 10. Elastic mode shape of the printing press at 40 Hz. The degrees of freedom of the main drive motor and the intermediate gear are not shown.

by the compensation algorithm, as was the case in the simulation. The amplitudes of the other orders remain the same. This is also the case for the measured register variation where only the order 0.06 is influenced by the compensation.

Table 1 shows a summary of the results for direct comparison. The erroneous torque on the order of magnitude of 100 Nm generates a register variation of several μm in the measurement as well as in the simulation. Both simulation and measurement show the proportional relationship between torque and register variation.

		amplitude motor torque order 10.06	amplitude register variation order 0.06
simulation	without compensation	97.2 Nm	5.4 μm
	with compensation	17.0 Nm	0.9 μm
	reduction	83%	83%
measurement	without compensation	92.2 Nm	7.1 μm
	with compensation	5.6 Nm	0.4 μm
	reduction	94%	93%

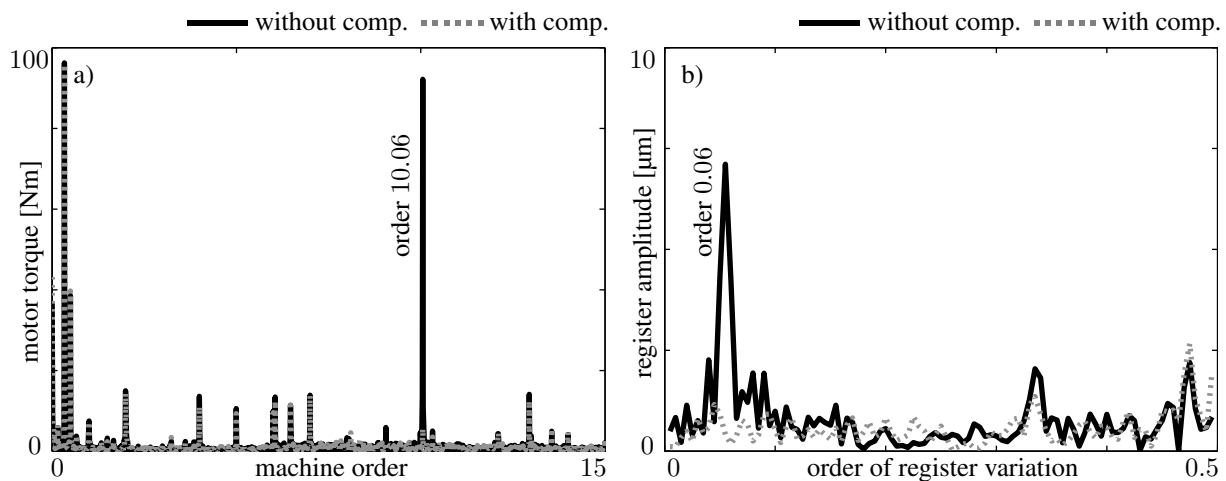Table 1. Summary of the simulation and measurement results.

Figure 11. a) Measured amplitude spectrum of the motor torque in machine coordinates [Nm] without and with compensation of the rotary encoder error. b) Measured amplitude spectrum of the register variation from 100 consecutive sheets [µm] without and with compensation of the rotary encoder error.

5 Summary and Conclusions

Using the presented mechanical model in conjunction with the post-processing sheet-tracking algorithm, it is possible to predict the effect of mechanical or control-related changes on the sheetfed offset printing press directly with regard to print quality. The method is suitable for steady-state printing at constant printing speed but also for transient processes such as emergency stop. The comparison of simulation and measurement in a case study shows a good agreement. In the range of a few µm, the effects of vibration excitations on the printed image can be predicted. These predictions can ultimately save time and money in machine development and production.

References

Brandenburg, G.: *Über das dynamische Verhalten durchlaufender elastischer Stoffbahnen bei Kraftübertragung durch Coulomb'sche Reibung in einem System angetriebener, umschlungener Walzen.* Dissertation TU München, München (1971).

Brandenburg, G.: *Verallgemeinertes Prozessmodell für Fertigungsanlagen mit durchlaufenden Bahnen und Anwendung auf Antrieb und Registerregelung bei Rotationsdruckmaschinen*, vol. 1(46). VDI-Verlag, Düsseldorf (1976).

Brandenburg, G.: New mathematical models and control strategies for rotary printing presses and related web handling systems. *IFAC Proceedings Volumes*, 44, (2011), 8620–8632.

Buck, B.; Knopf, E.; Schreiber, S.; Seidler, M.: Nichtlineare Schwingungsphänomene in Bogenoffsetdruckmaschinen. *VDI-Berichte*, Nr. 1917, (2005), 345–361.

Dresig, H.; Holzweißig, F.: *Maschinendynamik*. Springer-Verlag, Berlin Heidelberg (2009).

Galle, A.: *Regelungstechnische Untersuchung der Bedruckstoffförderung in Rollendruckmaschinen*. TU Chemnitz, Chemnitz (2007).

Heiler, P.; Hieronymus, J.: Farbwerk einer Druckmaschine. *Patent DE 102009008778 A1*, (2009).

Hummel, P.; Ortner, R.; Hinz, M.: Farbwerk für eine Rotationsdruckmaschine. *Patent DE 19715614 A1*, (1998).

Kipphan, H.: *Handbuch der Printmedien: Technologien und Produktionsverfahren*. Springer-Verlag, Berlin Heidelberg (2000).

Langer, P.: Bestimmung der Übertragungsgüte von Riementrieben. *VDI-Berichte*, Nr. 2197, (2013), 129–140.

Markert, R.: *Strukturdynamik*. Shaker, Aachen (2013).

Messer, M.: Parametererregte Drehschwingungen im Antriebsstrang von Bogenoffsetdruckmaschinen. *VDI-Berichte*, Nr. 2197, (2013), 1–12.

Norrick, N.: Statistical consideration of uncertainties in bolted joints of the drive train of sheet-fed offset printing presses. *Applied Mechanics and Materials*, 807, (2015), 3–12.

Polygraphische innovative Technik Leipzig GmbH: Produktdatenblatt Passer-Messsystem Luchs III and Pitsid. (2016).

Schnabel, H.: *Entwicklung von Methoden zur Registerregelung in Abhängigkeit der Bahnzugkraft bei Rollen-Tiefdruckmaschinen*. Sierke-Verlag, Göttingen (2009).

Wiese, H.: Antriebsdynamische Untersuchungen an Bogenoffsetmaschinen. *VDI-Berichte*, Nr. 1416, (1998), 105–118.

Wolfermann, W.: Tension control of webs - a review of the problems and solutions in the present and future. In: *Proceedings of Third International Conference on Web Handling*, pages 198–228, Stillwater, Oklahoma (1995).

Zitt, H.: *Entwicklung einer Modell-Bibliothek zur Simulation von Bahnspannung und Tänzerbewegung beim Transport von Materialbahnen*. Dissertation Universität des Saarlandes, Saarbrücken (2001).

Address: Nicklas Norrick, Heidelberger Druckmaschinen AG, Alte Eppelheimer Str. 26, 69115 Heidelberg, Germany
email: `nicklas.norrick@heidelberg.com`